Received: 18 July 2016 | Revised: 5 October 2016 | Accepted: 1 November 2016
DOI 10.1002/rcs.1792

WILEY The International Journal of Medical Robotics and Computer Assisted Surgery

ORIGINAL ARTICLE

A combined registration and finite element analysis method for fast estimation of intraoperative brain shift; phantom and animal model study

Amrollah Mohammadi[1] | Alireza Ahmadian[1,2] | Shahram Rabbani[3] | Ehsan Fattahi[4] | Shapour Shirani[3]

[1] Department of Medical Physics & Biomedical Engineering, School of Medicine, Tehran University of Medical Sciences, Tehran, Iran
[2] Research Centre for Biomedical Technology and Robotics (RCBTR), Tehran, Iran
[3] Tehran Heart Center, Tehran University of Medical Sciences, Tehran, Iran
[4] Department of Neurosurgery, School of Medicine, Tehran University of Medical Sciences, Tehran, Iran

Correspondence
Dr. Alireza Ahmadian, Professor of Biomedical Engineering, Poursina Ave, Keshavarz Blvd, Tehran, Iran. IR 14176-53761
Email: ahmadian@sina.tums.ac.ir

Funding information
Tehran University of Medical Sciences, Grant/Award Number: 91-04-30-20132; Research Center for Biomedical Technology and Robotics; Tehran Heart Center

Abstract

Background Finite element models for estimation of intraoperative brain shift suffer from huge computational cost. In these models, image registration and finite element analysis are two time-consuming processes.

Methods The proposed method is an improved version of our previously developed Finite Element Drift (FED) registration algorithm. In this work the registration process is combined with the finite element analysis. In the Combined FED (CFED), the deformation of whole brain mesh is iteratively calculated by geometrical extension of a local load vector which is computed by FED.

Results While the processing time of the FED-based method including registration and finite element analysis was about 70 s, the computation time of the CFED was about 3.2 s. The computational cost of CFED is almost 50% less than similar state of the art brain shift estimators based on finite element models.

Conclusions The proposed combination of registration and structural analysis can make the calculation of brain deformation much faster.

KEYWORDS
brain shift, CFED, FED registration, finite element analysis

1 | INTRODUCTION

Deformation of soft-tissue due to the surgical operation is one of the key challenges facing image-guided neurosurgery because it causes a misalignment between the actual position of pathology and its position in preoperative images. Craniotomy-induced brain shift is usually the first distortion of preoperative anatomy. Intraoperative imaging is widely used for surgical navigation but the imaging modalities that can be used intraoperatively do not have sufficient quality to confidently locate the lesions and critical normal areas. During the past two decades, many studies were carried out that tried to warp high quality preoperative images to the intraoperative position of the brain. The earlier ones were based only on registering intraoperative images to preoperative ones which may have been acquired by another imaging modality.[1–4] The more recent studies are focused on using biomechanical models of the brain that are loaded by the displacements extracted from intraoperative images in order to predict volumetric deformation of the brain.[5–12] Nevertheless, efforts continue for compensating soft-tissue deformation based only on image registration.[13] A clinical study for comparison of methods[14] indicates that biomechanical modeling can result in more accurate estimation of brain shift.

The biomechanical model widely used is a linear finite element model (FEM) in which the brain deformation is assumed to be infinitesimally small, i.e. the equations of solid mechanics are integrated over the initial brain geometry.[5,7,12] However the use of a nonlinear FEM to predict larger brain deformations has been of interest for several researchers.[8,10] Whiles the nonlinear biomechanical models facilitate more accurate prediction of the brain deformation at the expense of high computation time, the problems such as craniotomy-induced brain shift can be solved by a simple linear elastic model of brain tissue.[15]

As well as accuracy and reliability of the brain shift compensation methods, the adjustment of them to real-time constraints of neurosurgery has been gradually attended in several studies. It has been reported in earlier studies that linear finite element models can have lower computation times, around 80 s[16] and 15 s.[17] Joldes *et al.*[10] reported a reduction of time by about one order of magnitude (40 s to 4 s) by implementing a specialized nonlinear finite element algorithm on a graphic processing unit (GPU) instead of personal computer. In a more recent study, Sun *et al.*[18] reported a time of about one minute for inverse biomechanical modeling based on an atlas of all possible brain deformations created before the operation.

In the realistic conditions of an operating room, the overall procedure of correcting brain shift includes many tasks other than biomechanical model updating, and their time requirements usually are not reported (except some studies such as [18]). The FEM is driven by the sparse displacement vectors which result from registration of intraoperative data to preoperative images. Point-based rigid registration algorithms such as iterative closest point (ICP)[19] have been widely used to compute nodal displacements. Time requirements of rigid registration methods are negligible but they support only low deformations. Non-rigid point matching methods have been developed recently and employed in several studies.[5,12] Generally-developed non-rigid registration algorithms[20,21] are more complex and their computation time rapidly increases with the number of points.[21] Therefore, the traditional methods in which the calculation of nodal displacements and finite element analysis (FEA) are two distinct tasks may take more time than reported times for prediction of brain shift.

In our previous work[22] we followed the traditional method for estimation of brain shift but with a new registration method, finite element drift (FED). FED is a non-rigid matching algorithm in which the source points are nodes of a linear elastic model that are smoothly moved toward the target points to maximize the likelihood in a Bayesian framework. FED uses mechanical parameters of the model and is more consistent with the underlying nature of the deformed object. FED showed acceptable results in the calculation of local deformations compared with the well-known algorithm, coherent point drift (CPD).[21] Using FED registration the local displacements of cortical surface and internal vascular tree were calculated and applied to FEA software.

In the present work we propose a combination of registration with FEA to shorten the procedure of calculating volumetric deformation. Using this method any registration tasks related to different intraoperative imaging modalities and the FEA can be performed concurrently. It is expected that the proposed method can speed up the overall procedure of estimating brain shift.

To validate our proposed method an animal study was performed. This step is necessary before applying human experiments. Four dogs were selected for head surgery and after doing craniotomy and data acquisition they recovered safely. All our experiments on dogs were carried out under European Union regulations; 'Directive 86/609/EEC'[23] for the protection of animals used for experimental and other scientific purposes.

In the rest of the paper, we first explain the method of combining registration and FEA and then the procedures for preparing animals, processing pre- and intra-operative images, applying the method and finally calculating target registration error as a measure of estimation accuracy. Results obtained for the animal model will be presented in detail and discussed.

2 | MATERIALS AND METHODS

2.1 | Proposed combined FED

2.1.1 | Background

Here we present a quick review of the FED registration algorithm. A detailed description can be found in.[22] The FED registration algorithm is based on CPD method[21] in which the alignment of two point sets is considered as a probability density estimation problem, where one point set represents the Gaussian mixture model (GMM) centroids and the other one the data points. The maximum of GMM posterior probability is obtained when the two point sets are matched. The following notation is employed:

D: the dimension of point set (2 or 3)

$\mathbf{x}_1,\ldots,\mathbf{x}_N$:points in first point set (data points)

$\mathbf{y}_1,\ldots,\mathbf{y}_M$:points in second point set (GMM centroids)

$\mathbf{T}(\mathbf{y}_m, \theta)$: transform T applied to $\mathbf{y}_m$, where θ is the set of transformation parameters

In the non-rigid CPD method, the transformation of $\mathbf{y}_m$ points is defined as follows:

$$T(Y, v) = Y + v(Y) \tag{1}$$

where Y is the matrix of all $\mathbf{y}_m$ points, and $v(Y)$ is a smooth function that drifts $\mathbf{y}_m$ points toward the $\mathbf{x}_n$ points.

For FED method if $\mathbf{y}_m$ points are considered as the nodes of a linear elastic model (LEM), a small movement will be:

$$\Delta Y = K^{-1}F \tag{2}$$

where $Y_{MD\times 1} = \left(\boldsymbol{y}_1^T, \ldots, \boldsymbol{y}_M^T\right)^T$ is a column vector with $M \times D$ elements, K is the stiffness matrix and F is the load vector. Proper constraints on the LEM should be applied to generate a non-singular K matrix. This can be achieved when the number of supports or fixed nodes in the model is greater than those of moving nodes. The transformation will be as follows:

$$T(\mathbf{y}_m, \theta) = \mathbf{y}_m + K_m^{-1}F \tag{3}$$

where K_m^{-1} is a $D \times MD$ matrix of rows of K^{-1} corresponding to $\mathbf{y}_m$. The F vector, which minimizes the negative log-likelihood, should satisfy the following equation[22]:

$$\sum_{n=1}^{N}\sum_{m=1}^{M}\boldsymbol{P}^{old}(m|\boldsymbol{x}_n)\boldsymbol{K}_m^{-1T}\left(\boldsymbol{x}_n - \boldsymbol{y}_m - \boldsymbol{K}_m^{-1}\boldsymbol{F}\right) = 0 \tag{4}$$

After computing for F, the best σ^2 can be obtained by equating the corresponding derivative of Q to zero:

$$\sigma^2 = \frac{1}{N_p D}\sum_{n=1}^{N}\sum_{m=1}^{M}\left\|\boldsymbol{x}_n - \boldsymbol{y}_m - \boldsymbol{K}_m^{-1}\boldsymbol{F}\right\|^2 \tag{5}$$

Equations 4 and 5 are the M-step of the EM algorithm. In our previous work,[22] we did not present a direct solution of these equations but in here we rewrite Equation 4 to a matrix format which can be easily solved for load vector $\mathbf{F}$:

$$\boldsymbol{K}^{-1T}\boldsymbol{P}_e\boldsymbol{X} - \boldsymbol{K}^{-1T}d(\boldsymbol{P}_e 1)\boldsymbol{Y} - \boldsymbol{K}^{-1T}d(\boldsymbol{P}_e 1)\boldsymbol{K}^{-1}\boldsymbol{F} = 0 \tag{6}$$

If we consider the posterior probabilities matrix $\mathbf{P}$ with elements of $p_{mn} = \mathbf{P}^{old}(m|\,\mathbf{x}_n)$, the matrix $\mathbf{P}_e$ is an extension of P in which p_{mn} is replaced by:

$$p_{e(mn)} = p_{mn} * \textit{identity matrix of size } D \tag{7}$$

Thus $\mathbf{P}_e$ is a $MD \times ND$ matrix. $d()$ denotes a diagonal matrix and '**1**' is a column vector of ND ones. Also $\mathbf{Y}_{MD\times 1} = \left(\mathbf{y}_1^T, \dots, \mathbf{y}_M^T\right)^T$ and $\mathbf{X}_{ND\times 1} = \left(\mathbf{x}_1^T, \dots, \mathbf{x}_N^T\right)^T$ are column vectors of source and target points, respectively.

Equation 6 can be easily solved for $\boldsymbol{F}$ as:

$$\boldsymbol{F}_i = \boldsymbol{K}\times\left(d(\mathbf{P}_e 1)^{-1}\mathbf{P}_e\boldsymbol{X}-\boldsymbol{Y}\right) \tag{8}$$

This equation is a straightforward solution for load vector $\boldsymbol{F}$. The subscript '*I*' denotes iteration i of the FED algorithm.

2.1.2 | Overall procedure

Figure 1 shows a detailed schematic diagram of the overall procedure proposed for calculating brain deformation by the CFED algorithm. Preoperative MR and MR angiography (MRA) images are processed to extract the main brain segments and vascular tree, respectively. The 3D image of brain is meshed such that the points on vessels are considered as nodes of the mesh. After constructing a stiffness matrix of the whole brain mesh, some nodes to be registered by FED algorithm to intra-operatively captured point sets, are selected to build a smaller matrix $\boldsymbol{K}_f$. In our study, the nodes that were the source points ($\boldsymbol{Y}$) for FED were chosen as the nodes on vessels near pathology and surface nodes in the craniotomy area. The sub-matrix $\boldsymbol{K}_f$ is a portion of the original matrix $\boldsymbol{K}$ and can be easily separated from it.

In the operating room, the point clouds should be made using intra-operative imaging modalities to be applied to FED algorithm as target points. In our study these points were captured by scanning our previously proposed projected landmarks on cortical surface ($\boldsymbol{X}_s$) and the points on deformed vascular tree that were extracted by the localized 2D Doppler ultrasound images ($\boldsymbol{X}_d$). In each iteration of the FED algorithm the optimum load vector $\boldsymbol{F}_i$ is computed and then extended to all nodes of the mesh. The displacements of all mesh nodes are iteratively calculated using this vector and $\boldsymbol{K}$. The deformed brain mesh can be used to warp preoperative images in a navigation system.

2.1.3 | Building stiffness matrices

After smoothing the 3D image and meshing it, the stiffness matrix of the whole mesh is constructed. We used the direct stiffness method (DSM) of structural analysis which is by far the most common implementation of the finite element method.[24,25] In particular, all the main commercial finite element analysis codes are based on DSM. The stiffness matrix ($\boldsymbol{K}$) will be a real symmetric matrix. For a 3D mesh with N nodes the matrix $\boldsymbol{K}$ will have $3\ N \times 3\ N$ elements.

After constructing stiffness matrix of the mesh, some nodes that should be registered with the FED algorithm can be selected to build a smaller matrix $\boldsymbol{K}_f$. This matrix is a portion of the original matrix $\boldsymbol{K}$ and can be easily separated from it. According to the rules of DSM, if two or more sets of isolated nodes are picked for FED (as our approach to combine internal vessels and surface displacements) the matrix $\boldsymbol{K}_f$ may be composed of two separate square matrices placed diagonally and other elements are zeroes (Figure 2).

2.1.4 | Geometrically extending FED result to whole mesh

The matrix $\boldsymbol{K}$ in Equation 8 is the same $\boldsymbol{K}_f$ which is picked up from the whole mesh matrix $\boldsymbol{K}$. For geometrically extending the registration results to the whole mash, the $\mathbf{y}$ points which are the moving nodes of the FE mesh are loaded by $\boldsymbol{F}$ and all other nodes are considered untouched. Therefore the load vector can be extended to all mesh nodes by inserting zeroes for the remaining nodes. Therefore the displacement of all mesh nodes can be calculated as:

$$\Delta \boldsymbol{Y}_{t_i} = \boldsymbol{K}^{-1}\boldsymbol{F}_{t_i} \tag{9}$$

where $\boldsymbol{F}_{t_i}$ is the extended load vector for the i'th iteration of CFED and $\boldsymbol{Y}_t$ is the vector of all mesh nodes. Using this equation the brain

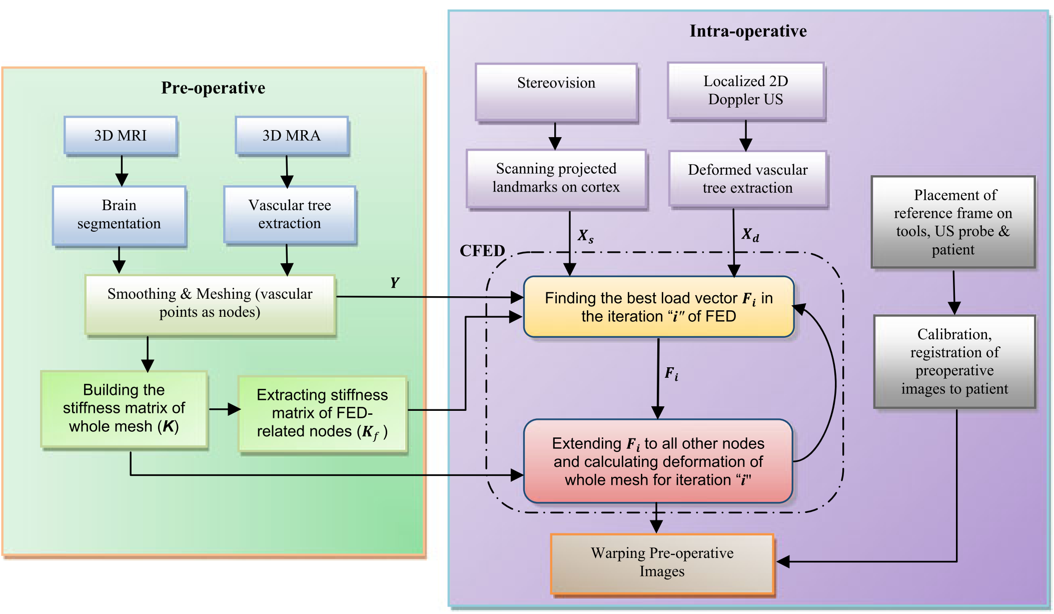

FIGURE 1 Schematic view of overall procedure and CFED algorithm

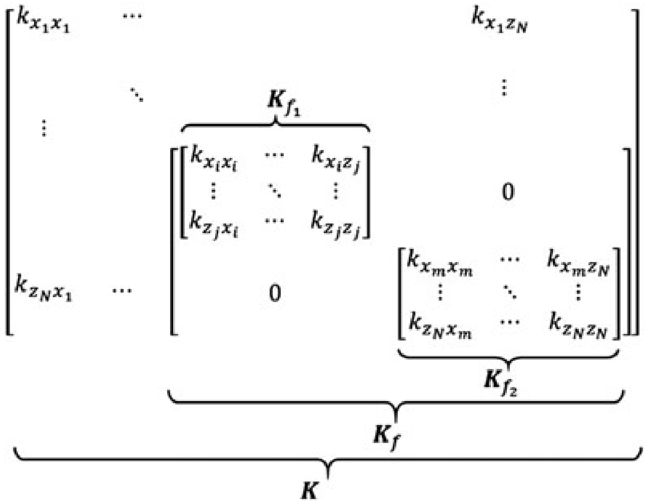

FIGURE 2 An example of stiffness matrices of whole mesh (K) and FED-related nodes (Kf). Kf contains two sets of isolated nodes (Kf1 and Kf2)

deformation is smoothly computed in each iteration of CFED. Because the matrix $\boldsymbol{K}^{-1}$ is considered to be invariant for low deformations[15] of a LEM, calculation of $\Delta \boldsymbol{Y}_t$ will be fast. Also the $\boldsymbol{K}$ is a real symmetric matrix which can be easily inverted using Cholesky decomposition at the initial step of the algorithm.

2.1.5 | Speed improvement

After implementation of the CFED algorithm in the MATLAB environment we tried to optimize its speed. Application of some approximations can reduce the computational complexity of the method. The fast Gaussian transform (FGT) and low-rank matrix approximation which were proposed by the CPD authors[21] were used to speed up CFED. The codes provided for these methods in[21] were applied to the CFED algorithm and their effects on speed and accuracy were tested. Obviously the speed increases at the expense of a slight reduction of accuracy. We named the algorithm with these two modifications the fast CFED.

2.2 | Brain phantom

The captured data sets from the brain phantom in different deformation states in our previous work[22] were accurately recalled and reprocessed. The primary goal was a comparison of computation times and accuracy of the CFED method compared with the previously used FED-based method. The mesh size and the number of nodes included in FED registration were the same for both approaches and all data sets. The mesh had 7152 tetrahedral elements and 220 nodes were candidates for FED. There were five series of data for each inflation volume, 5 and 10 mL. Smoothing and meshing the volume were performed in MATLAB software for both methods. The time required for FED registration plus FEA was considered as the total computation time of the previous method that should be compared with the computation time of the new CFED algorithm. The finite element analysis software was an open-source code, Calculix[1] that was customized for our study.

[1]http://www.calculix.de/

TABLE 1 The age, weight of dogs and type of object inserted inside the brain

ID	age (years)	weight (kg)	target type
Dog1	3.5	19.4	3 mL water
Dog2	0.9	17.2	3 mL blood (hematom)
Dog3	2.5	20.3	coated TNG pills
Dog4	5	22.5	coated TNG pills

Points on the center line of tubes inside the phantom were considered as target points and mean displacement of them was defined as target shift. The absolute shift and the accuracy of shift estimation were calculated by rigid registration of post-inflation MR images to pre-inflation ones and deformed brain meshes respectively.

2.3 | Animal model

We had one set of animal data that was gathered from our experiments on a dog.[22] We named that dog Dog1 and three more dogs that were used for the present study as Dog2, Dog3 and Dog4. Before each operation the skull of the animal was drilled to insert a tumor-like object inside the brain tissue as the target of brain shift estimation. Table 1 shows the age and weight of dogs and the target type utilized for each of them. The spherical pills of trinitroglycerin (TNG) that were used for Dog3 and Dog4 created bright circles in MR images and could be easily segmented. The pills were coated with a waterproof layer that would not dissolve during the operation.

The preoperative MR images were taken with a SIEMENS Avanto[2] 1.5 T scanner, and a standard T1-wieghted scanning sequence at a voxel resolution of 0.78 × 0.78 × 0.8 mm was applied. Also acquisition of 3DTOF MRA images were performed without injection of any agents. In the operating room, a stereo camera was calibrated and utilized for acquiring 3D positions of reference frames on tools, ultrasound (US) probe and also projected landmarks over the cortex surface. It was the same Micron Tracker of Claron, Inc., under Parsiss Image-Guided Navigation[3] which was used in the previous studies conducted by our group.[26,27] Before craniotomy, the head of the animal was rigidly registered to preoperative MR images.

After craniotomy and duratomy, a checkerboard pattern was projected on the visible surface of the cortex and cross-points of the projected pattern were scanned by a stereo camera to calculate their 3D positions. Also 2D Doppler US images were acquired by a probe that was swept over parenchyma and tracked by the camera. A detailed description of the surface scanning method and other procedures of data acquisition can be found in our previous work.[22] For Dog2 due to its unstable conditions in heart rate and blood pressure, the Doppler US imaging did not give meaningful data and only surface data was used. After recording intraoperative data, the animal with an

[2]https://www.healthcare.siemens.com/magnetic-resonance-imaging/0-35-to-1-5t-mri-scanner/magnetom-avanto

[3]Parseh Intelligent Surgical Systems Parsiss Company, Tehran, Iran. www.parsiss.com.

TABLE 2 The number of tetrahedral elements, surface nodes in craniotomy area, nodes on vascular tree, remaining points on the scanned surface after preprocessing and finally the points on the deformed vascular tree

ID	Mesh elelementss	Surface nodes	Vascular nodes	Nodes around the target	Points on deformed surface	Points on deformed vascular tree
Dog1	3718	170	102	147	1630	233
Dog2	3220	152	84	115	1380	NA
Dog3	4082	210	136	77	1900	387
Dog4	3890	194	122	84	1720	425

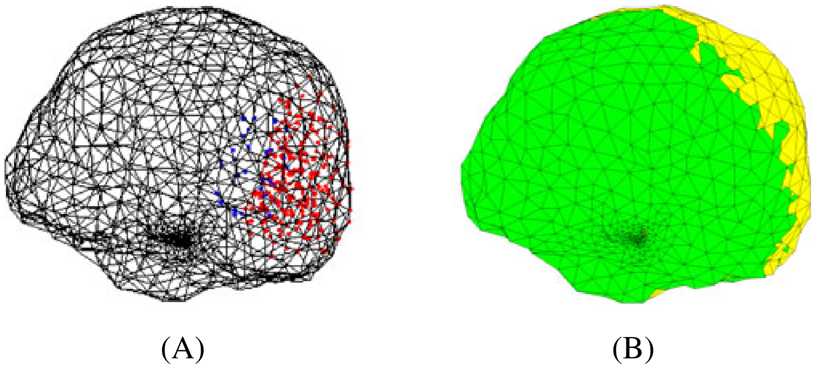

FIGURE 3 A, Meshed brain of Dog1; surface (red) and vascular (blue) nodes picked up for FED. B, The overlapped mesh before (green) and after (yellow) running the proposed method

opened skull was directed to the MR imaging machine to acquire images that were used for validating our brain shift estimator.

Using 3DSlicer software,[28] the preoperative MR images processed to segment brain to its principal parts. A reference database of dog anatomy[29] was used to perform manual segmentation carefully. The software developed by our group[26,27] was used to filter the outliers and duplicated points from the 3D point cloud of the cortical surface. Also the same methods described in our previous study[22] were applied to MRA and Doppler US images to extract minimum vasculature around the tumor.

The surface of the 3D image of the brain was smoothed such that an approximately uniform surface mesh was obtained. The meshing of volume started from the surface. The points corresponding to the vascular tree were used as nodes of the mesh. Using this method, there was no need to find nearest nodes to vessels, as performed in our previous study.[22] Points which were placed more closely to others, less than 10% of the mean nodal distance, were omitted to obtain an approximately uniform mesh. The final size of mesh for each brain, the number of nodes in the craniotomy area, nodes on the vascular tree and nodes placed around the target are shown in Table 2. Also the number of points that were extracted from intraoperative images and processed to represent the deformed surface and vessels can be found in Table 2.

Three methods were applied to each data set of animals to compute the deformation of the brain; a previously used FED-based method with FED registration and FEA tasks, the proposed CFED and the fast CFED method. To reach a better record for the previously used method, we combined surface and vessels registrations in one FED task, as applied in the new method. Figure 3 shows the meshed brain of Dog1 and the nodes marked as inputs to FED. Also an overlapped image of the mesh before and after running the new method is shown in this figure.

We defined the distance between the gravity centers of the tumor before and after craniotomy as brain shift. The absolute shift and the accuracy of shift estimation were calculated by rigid registration of post-craniotomy MR images to preoperative ones and deformed brain mesh respectively.

3 | RESULTS

The machine which was used to process data was a desktop computer with Core i7 (4790 K) CPU with up to 4.4 GHz speed, 16GB RAM and 1 TB hard disk drive. Except FEA software, other codes were implemented in MATLAB.

3.1 | Phantom study

The absolute shifts that were induced by 5 and 10 mL inflation of internal balloon were measured as 7.1 ± 0.4 and 9.5 ± 0.7, respectively. Mean errors of shift estimation after processing by previous FED-based, new CFED and fast CFED methods as well as computation time of each method are shown in Table 3.

The results show that computation time of CFED method was less than 25% to 30% of the previous FED-based method. Also the estimation errors were decreased by up to 5% by the new algorithm. We will discuss this further achievement in the discussion section. The results of fast CFED indicate one order of magnitude reduction in

TABLE 3 Mean errors of shift estimation using FED-based, CFED and fast CFED methods and computation time of each method in two inflation cases of the baloon inside the phantom, 5 and 10 mL

	Mean error (mm)		Computation time (s)	
	5 ml	10 ml	5 ml	10 ml
FED-based	1.31 ± 0.31	1.43 ± 0.36	78 ± 8	105 ± 12
CFED	1.24 ± 0.26	1.36 ± 0.30	20 ± 3	31 ± 5
Fast CFED	1.38 ± 0.33	1.50 ± 0.41	5.3 ± 0.9	7.1 ± 1.3

computation time with a negligible loss of accuracy. Figure 4 shows box plots of results that are shown in Table 3. The results indicate that when the deformation increased due to the inflation, the estimation error and time of process slightly increased.

3.2 | Animal model study

The measured and mean errors of estimating brain shift using three named methods as well as their computation times are shown in Table 4. The combination of surface and vessels data was used to calculate craniotomy induced brain shift except for Dog2 because Doppler US data were unusable. Figure 5 shows a box plot representation of the results in Table 4.

Comparison of mean errors in Table 4 indicates that the CFED method outperforms the previous FED-based method by up to 5% in average registration error. The main achievement is that this modification has led to reduction of the total computation time by 70%. The results clearly prove that the fast CFED method can be utlized in a real-time procedure which is the current need for image guided neurosurgery systems. As shown the brain deformation can be computed in an average time of 3.2 s which is much faster than both FED-based and CFED methods. The error growth with fast CFED averages less than 0.2 mm, which does not exceed 3% of the total brain shift.

4 | DISCUSSION

The main goal of this study was to improve the speed of calculation of brain deformation by simplification of the structural analysis in combination with image registration. In our previous work the two processes of registration and finite element analysis were performed separately. This caused a heavy computational cost thus making the algorithm not suitable for real-time analysis in the operating room. In this study we managed to combine the registration process with structural analysis leading to a much faster algorithm for brain shift calculation.

Also the experimental study in previous work was performed only on one animal data, but for the present study three new dogs underwent our experimental test in order to evaluate the proposed CFED method more precisely. The computation time of the finite element analysis in the CFED method was reduced but the FED registration was found to be a time-consuming process. For further improvement of overall speed of the algorithm, we used some computational tricks to further reduce the complexity of FED. The computation times of the fast version of the CFED method are comparable with reported times for similar state of the art brain shift estimators. Among recent studies on brain deformation prediction only a few reported computation times. Joldes *et al.*[10,30] reported a time less than 4 s to perform a finite element analysis of a mesh with about 17000 elements. Sun *et al.*[18] proposed an inverse modeling based on a pre-computed atlas of all possible brain shifts. It took 1 min for registration and 1 min for inverse modeling with their method. A competitive comparison of the computational cost of our approach and these most recent studies is shown in Table 5. The computational cost of fast CFED is almost 50% less than the FEM-based method proposed in[30] while the time requirement for image registration was not included in their records. The proposed method[18] has less computational cost because the deformation calculations had been performed for about 12 h before operation.

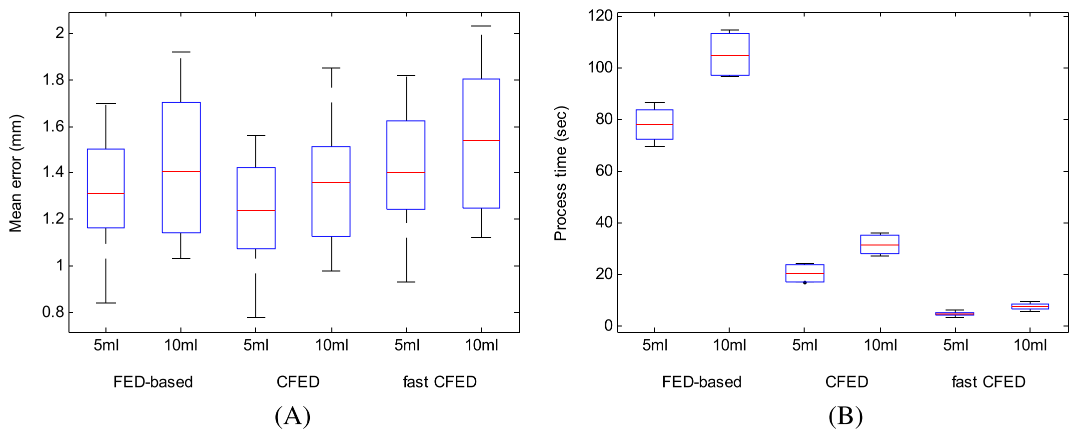

FIGURE 4 Box plots of A, mean error of shift estimation and B, computation time of FED-based, CFED and fast CFED methods

TABLE 4 Mean error of brain shifts estimation

	Measured brain shift (mm)	Mean estimation error (mm)			Computation time (s)		
		FED-based	CFED	Fast CFED	FED-based	CFED	Fast CFED
Dog1	6.7	1.55	1.47	1.61	76	22	3.1
Dog2	4.4	1.64	1.56	1.80	48	14	2.7
Dog3	7.2	1.36	1.28	1.44	85	26	3.5
Dog4	7.5	1.72	1.66	1.75	74	24	3.5
Average	6.5 ± 1.46	1.57 ± 0.15	1.49 ± 0.16	**1.65 ± 0.16**	70 ± 16	21.5 ± 5	**3.2 ± 0.4**

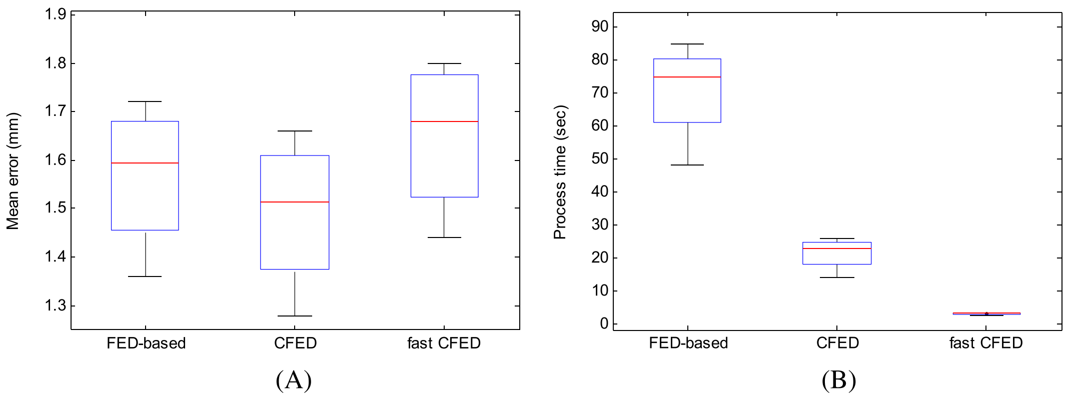

FIGURE 5 Box plots of A, mean error of shift estimation and B, computation times of FED-based, CFED and fast CFED methods

TABLE 5 Comparison of computaional cost of fast CFED with other methods

	CPU: speed (GFLOPS*)	Elements	Time (s)	Cost (GFLOPS × s/ elements)
Joldes *et al.* (2010)[30]	Nvidia Tesla c870 GPU: (~384)	16 825	3.54	0.081
Sun *et al.* (2014)[18]	Intel Core i5: (~21)	100 000	120	0.025
Fast CFED	Intel Core i7: (~44)	3728	3.2	0.038

*GFLOPS : Giga floating point operation per second

The proposed CFED method has made several assumptions which should be noted. The first assumption is the linearity of the model. It might be widely thought that every patient-specific finite element model must suffer from uncertainties of non-linear mechanical properties of the brain tissue. The results of a parametric study[15] show that for deformations such as craniotomy-induced brain shift which do not include topology changes (e.g. cutting, tissue removal) or surgical tool forces, one can use the simplest linear elastic model (LEM) with any reasonable value of Young's modulus and Poisson's ratio close to 0.5. Therefore it can also be assumed that the stiffness matrix (K) of our LEM is invariant during the iterations of CFED. On the other hand the model can be considered geometrically linear because the source points (nodes) smoothly drifted towards target points leading to small geometric changes in each iteration. This could be the reason for a little accuracy improvement. However the accuracy improvement is interpreted by averaging the measurements of brain shift. It should be mentioned that the accuracy of computing absolute brain shift is limited by the voxel size of MRI (0.78 mm).

Another assumption we made is that the nodes which become a candidate for FED are close to each other and the generated mesh connects them. Therefore the $\boldsymbol{K_f}$ matrix can be easily separated from $\boldsymbol{K}$. If such nodes are sparsely placed in the mesh, the $\boldsymbol{K_f}$ contains unwanted nodes. Although the larger matrix may reduce the speed of the registration algorithm the FED considers undesired nodes as outliers and the total process is not affected.

Some procedures related to capturing intraoperative data, filtering noise and outliers, 3D visualization of Doppler US and many other preprocesses that were mentioned in our previous work[22] are time-consuming tasks. The total time required for these procedures may be greater than the time of biomechanical modeling.[18] Other limitations such as the light adjustment in operating room for a reliable surface scan or capturing useful Doppler US images from vasculature around the pathology remain in our proposed method and should be solved before clinical application. However our animal study indicates that the proposed fast CFED with a combination of intraoperative imaging modalities can result in quick and reliable estimation of brain shift.

5 | CONCLUSIONS

In the present study, we attempted to solve the biggest problem of excessive time consumption in the FEM-based methods, that designated to estimate the intraoperative brain shift. Our approach was a combination of registration and finite element analysis that could speed up the entire process. Our previously proposed FED registration method and the FEA are both based on a linear elastic model and we combined them in an iterative algorithm.

Our experiments on a phantom and an animal model indicated that the CFED method reduced the computational cost by almost 70%. Besides speed enhancement, the smooth movement of loading nodes can preserve linearity of the model and consequently makes the structural analysis more accurate. The results showed an improvement about 5% in final accuracy. Using some approximations, a fast version of CFED was developed which can compute brain deformation in a time less than 3.2 s with negligible degradation of accuracy.

This pre-clinical study is an initial attempt to introduce FEM-based methods as real-time applications usable in surgical navigation.

ACKNOWLEDGMENTS

This study has been funded by Tehran University of Medical Sciences, TUMS under the grant No: 91-04-30-20132, and was supported by the Research Center for Biomedical Technology and Robotics (RCBTR), and Tehran Heart Center, Tehran, Iran.

ETHICAL APPROVAL

All institutional and national guidelines for the care and use of laboratory animals were followed.

CONFLICT OF INTEREST STATEMENT

The authors declare that they have no conflict of interest.

REFERENCES

1. Chen SJ, Reinertsen I, Coupé P, et al. Validation of a hybrid Doppler ultrasound vessel-based registration algorithm for neurosurgery. *Int J Comput Assist Radiol Surg*. 2012 Sep 1;7(5):667–685.
2. Letteboer MM, Willems PW, Viergever MA, Niessen WJ. Brain shift estimation in image-guided neurosurgery using 3-D ultrasound. *Biomed Eng, IEEE Trans*. 2005 Feb;52(2):268–276.
3. Mercier L, Del Maestro RF, Petrecca K, et al. New prototype neuronavigation system based on preoperative imaging and intraoperative freehand ultrasound: system description and validation. *Int J Comput Assist Radiol Surg*. 2011 Jul 1;6(4):507–522.
4. Müns A, Meixensberger J, Arnold S, et al. Integration of a 3D ultrasound probe into neuronavigation. *Acta Neurochir*. 2011 Jul 1; 153(7):1529–1533.
5. Bucki M, Palombi O, Bailet M, Payan Y. Doppler ultrasound driven biomedical model of the brain for intraoperative brain-shift compensation: a proof of concept in clinical conditions. *Soft Tissue Biomechanical Modeling for Computer Assisted Surgery*. Studies in Mechanobiology, Tissue Engineering and Biomaterials Series, Springer2012;11:135–165. doi: 10.1007/978-3-642-29014-5
6. Clatz O, Delingette H, Talos IF, et al. Robust nonrigid registration to capture brain shift from intraoperative MRI. *Med Imag IEEE Trans*. 2005 Nov;24(11):1417–1427.
7. DeLorenzo C, Papademetris X, Staib LH, et al. Volumetric intraoperative brain deformation compensation: model development and phantom validation. *Med Imag, IEEE Trans*. 2012; Aug 31(8):1607–1619.
8. Hu J, Jin X, Lee JB, et al. Intraoperative brain shift prediction using a 3D inhomogeneous patient-specific finite element model. *J Neurosurg*. 2007 Jan;106(1):164–169.
9. Ji S, Liu F, Fan X, *et al*. Model-based brain shift compensation in image-guided neurosurgery. InSPIE Medical Imaging 2009 Feb 26 (pp. 72612E-72612E). International Society for Optics and Photonics.
10. Joldes G, Wittek A, Couton M, et al. Real-time prediction of brain shift using nonlinear finite element algorithms. Medical Image Computing and Computer-Assisted Intervention (MICCAI 2009). *Lecture Notes in Computer Science*. 2009;5762:300–307. doi: 10.1007/978-3-642-04271-3_37
11. Payan Y. *Soft Tissue Biomechanical Modeling for Computer Assisted Surgery*. Heidelberg, Berlin: Springer; 2012 Apr 27.
12. Zhuang DX, Liu YX, Wu JS, et al. A sparse intraoperative data-driven biomechanical model to compensate for brain shift during neuronavigation. *Am J Neuroradiol*. 2011 Feb 1;32(2):395–402.
13. Rivaz H, Chen SJ, Collins DL. Automatic deformable MR-ultrasound registration for image-guided neurosurgery. *IEEE Trans Med Imag*. 2015 Feb;34(2):366–380.
14. Garlapati RR, Roy A, Joldes GR, et al. More accurate neuronavigation data provided by biomechanical modeling instead of rigid registration. *J Neurosurg*. 2014 Jun;120(6):1477–1483.
15. Wittek A, Hawkins T, Miller K. On the unimportance of constitutive models in computing brain deformation for image-guided surgery. *Biomechan Model Mechanobiol*. 2009 Feb 1;8(1):77–84.
16. Skrinjar O, Nabavi A, Duncan J. Model-driven brain shift compensation. *Med Image Anal*. 2002 Dec 31;6(4):361–373.
17. Warfield SK, Talos F, Tei A, et al. Real-time registration of volumetric brain MRI by biomechanical simulation of deformation during image guided neurosurgery. *Comput Visualiz Sci*. 2002 Jul 1;5(1):3–11.
18. Sun K, Pheiffer TS, Simpson AL, et al. Near real-time computer assisted surgery for brain shift correction using biomechanical models. *IEEE Translation Eng Health Med*. 2014;2:1–3.
19. Besl PJ, McKay ND. Method for registration of 3-D shapes. In Robotics-DL tentative 1992 Apr 30 (pp. 586–606). International Society for Optics and Photonics.
20. Chui H, Rangarajan A. A new point matching algorithm for non-rigid registration. *Comput Vision Image Understanding*. 2003 Mar 31;89(2):114–141.
21. Myronenko A, Song X. Point set registration: coherent point drift. *Pattern Anal Machine Intell IEEE Trans*. 2010 Dec;32(12):2262–2275.
22. Mohammadi A, Ahmadian A, Azar AD, et al. Estimation of intraoperative brain shift by combination of stereovision and doppler ultrasound: phantom and animal model study. *Int J Comput Assist Radiol Surg*. 2015 Nov 1;10(11):1753–1764.
23. Directive C. 86/609/EEC of 24 November 1986 on the approximation of laws, regulations and administrative provisions of the Member States regarding the protection of animals used for experimental and other scientific purposes. *Off J Eur Commun*. 1986 Dec 18;29:L358
24. Felippa CA. Introduction to finite element methods. Course Notes, Department of Aerospace Engineeing Sciences, University of Colorado at Boulder, available at: http://www.colorado.edu/engineering/Aerospace/CAS/courses. d/IFEM. d. 2004
25. Miller FP, Agnes AF, McBrewster J. *Direct Stiffness Method*. Alpha Press; 2010.
26. Ahmadian A, Dadashi Serej N, Karimifard S, Farnia P. An efficient method for estimation of soft tissue deformation based on intra-operative stereo image features and point-based registration. *Int J Imag Syst Technol*. 2013;23(4):294–303. doi: 10.1002/ima.22064
27. Dadashi Serej N, Ahmadian A, Mohagheghi S, Sadrehosseini SM. A projected landmark method for reduction of registration error in image-guided surgery systems. *Int J Comput Assist Radiol Surg*. (JCARS), Springer: Published onlineMay 2014. doi: 10.1007/s11548-014-1075-z
28. Free and open source software package for visualization and medical image computing, Brigham and Women's Hospital, Harvard Medical School, http://www.slicer.org/
29. Evans HE. *De Lahunta A*. Elsevier Health Sciences: *Miller's Anatomy of the Dog*; 2013 Aug. 7.
30. Joldes GR, Wittek A, Miller K. Real-time nonlinear finite element computations on GPU–application to neurosurgical simulation. *Comput Methods Appl Mechan Eng*. 2010 Dec 15;199(49):3305–3314.

How to cite this article: Mohammadi, A., Ahmadian, A., Rabbani, S., Fattahi, E., and Shirani, S. (2016), A combined registration and finite element analysis method for fast estimation of intraoperative brain shift; phantom and animal model study, *Int J Med Robotics Comput Assist Surg*, doi: 10.1002/rcs.1792